Generation of sub-Poissonian light using active control with twin beams

J. Mertz, A. Heidmann, and C. Fabre
Laboratoire de Spectroscopie Hertzienne, Université Pierre et Marie Curie, Boîte Postale 74, F75252 Paris CEDEX 05, France
(Received 26 February 1991)

We present a general theory for intensity noise reduction when one beam of light is used to control another. We use a semiclassical input-output formalism and determine the conditions necessary for noise reduction below the shot-noise level. Configurations are examined where the intensity of one beam is monitored and control is effected directly to the other beam (feedforward), or indirectly through the beam source (feedback). The results are applied to the case of twin beams generated by an optical parametric oscillator. We detail for this system the implementation of an electro-optic control channel. Finally, a comparison is made between theory and experiment.

I. INTRODUCTION

Active control devices have long proved effective in reducing the fluctuations of various physical parameters, both in electronics and in optics. For example, systems controlling the intensity fluctuations of a laser beam by optoelectronic feedback are now widely used to reduce laser "technical" noise. The potential of such systems for reducing fluctuations of quantum origin, however, has only recently been recognized. Yamamoto and coworkers demonstrated using feedback techniques so that one could reduce, in a semiconductor laser, either its phase noise below the Schawlow-Townes limit [1] or its intensity noise below the shot-noise limit [2]. In the latter experiment, the generation of sub-shot-noise light required the monitoring of the total laser intensity to provide the feedback signal. This light, commonly referred to as sub-Poissonian or intensity squeezed, was restricted therefore to only the span between the laser and the detector and could not be extracted for external use. Several schemes were proposed for providing a feedback signal without destroying the controlled beam of interest. These included the use of the quantum nondemolition (QND) measurement [3,4] or of correlated beams [5–8].

The interest in correlated beams was first realized in the photon counting regime where the statistics of a photon flux were tailored in a closed-loop system, and sub-shot-noise light extracted using the twin photons emitted by an atomic cascade or by parametric fluorescence. The photon count rate of one beam was measured and the information used to react directly on the twin beam using gating techniques [9–13]. Experiments in this photon counting regime yielded modest amounts of quantum noise reduction [14] or very low photon fluxes [12–15] because of the poor quantum efficiency of photon counters. Similar experiments using analog photodetectors of high quantum efficiency have fared better. Intensity noise reductions of more than 20% have recently been reported, using linear control with parametric fluorescence [16] and optical parametric oscillation [17].

The purpose of this paper is to study to what extent intensity noise reduction is possible when active control is applied to correlated (or partially correlated) beams. A general theory will be presented for this noise reduction, from which we will concentrate on the actual implementation both of a correlated beam source and of an active control channel. In particular, we will examine the conditions necessary for the generation of sub-shot-noise light.

The general theory of noise control is developed in Sec. II, where we determine the optimal amount of noise reduction that may be obtained given any two beams. These beams will be specified only by their initial intensity correlations and respective intensity noises. A semiclassical input-output formalism [18] will be used since this is well adapted for control theory. In Sec. III, we will apply these general results to the specific case of twin beams generated by an optical parametric oscillator (OPO). As an extension of previous studies [8], we will determine for this system the optimal amount of noise reduction that is possible with active control. Extra losses and detunings will be included in our treatment of the OPO [19], which corresponds to the experimental situation [20–23] where the signal and idler fields are not perfectly correlated. Finally, in Sec. IV, we will detail how an active control can actually be implemented to attain this optimal noise reduction. The results of our experimental study will be presented alongside.

II. THEORY OF NOISE CONTROL USING TWO BEAMS

A. Basic model

We consider two fields to study to what extent the intensity fluctuations in one field (beam 1) can be controlled by monitoring the intensity of the second field (beam 2). We will consider a general control mechanism where the transfer of intensity information from one field to the other is linear. Particular examples of optoelectronic control mechanisms will be given in later sections.

We use here a semiclassical approach [18,24,25] where quantum field fluctuations are described by classical stochastic variables associated with the Wigner distribution. More precisely, the electric field operator a_i for each beam ($i=1,2$) is replaced by

$$\alpha_i(t)=\bar{\alpha}_i+\delta\alpha_i(t)\ , \tag{1}$$

where $\bar{\alpha}_i$ is the mean-field amplitude and $\delta\alpha_i(t)$ a classical random field that fits the Wigner distribution of the quantum fluctuations. The evolution of the field fluctuations is described then by classical equations linearized about the mean-field value. This method is closely connected to the standard linear stability analysis [26], and has been shown to be equivalent to the standard quantum linearization method for the case of parametric oscillators [18,27].

We will be interested only in intensity fluctuations given by

$$\delta I(t)=|\bar{\alpha}_i|\delta p_i(t)\ , \tag{2}$$

where δp_i are the amplitude fluctuations; that is, the fluctuations of the quadrature component in phase with the mean field. In the case where the mean fields are real, δp_i is equal to twice the real part of $\delta\alpha_i$.

The principal effect of a control mechanism is to correct the intensity fluctuations of beam 1 by a term proportional to the intensity fluctuations of beam 2. Neglecting various refinements which will be studied in later sections, such a correction can be modeled by

$$\delta\tilde{p}_1(t)=\delta p_1(t)-\int_{-\infty}^{+\infty}d\tau\, G(\tau)\delta p_2(t-\tau)\ . \tag{3}$$

The tilde here indicates *post* correction and $G(\tau)$ is a transfer function, assumed to be real and causal $[G(\tau<0)=0]$. In frequency space, this becomes

$$\delta\tilde{p}_1(\Omega)=\delta p_1(\Omega)-G(\Omega)\delta p_2(\Omega)\ , \tag{4}$$

where $G(\Omega)$ mediates the direct transfer of fluctuations from beam 2 to beam 1 at a frequency Ω.

The intensity noise spectrum of each beam is related to the amplitude fluctuations through

$$S_i(\Omega)=\langle\delta p_i(-\Omega)\delta p_i(\Omega)\rangle\quad(i=1,2)\ , \tag{5}$$

where S_i is equal to 1 when δp_i represents vacuum fluctuations; that is, for a coherent state. $S_i(\Omega)$ is thus normalized to the shot-noise level of each beam. We note here that, in the semiclassical approach, the fluctuations δp_i represent both the classical and quantum field fluctuations. $S_i(\Omega)$ less than 1 indicates that the fluctuations are smaller than the vacuum fluctuations whereas $S_i(\Omega)$ larger than 1 indicates the presence of extra classical noise.

The correlations between the two beams can be characterized by the function

$$C_{12}(\Omega)=\langle\delta p_1(-\Omega)\delta p_2(\Omega)\rangle\ . \tag{6}$$

Since $\delta p_i(t)$ and $G(\tau)$ are real functions, one finds

$$\begin{aligned}&\delta p_i^*(\Omega)=\delta p_i(-\Omega)\ ,\\ &G^*(\Omega)=G(-\Omega)\ ,\\ &C_{12}^*(\Omega)=C_{12}(-\Omega)=C_{21}(\Omega)\end{aligned} \tag{7}$$

obtaining a Cauchy-Schwartz inequality:

$$|C_{12}(\Omega)|^2\le S_1(\Omega)S_2(\Omega)\ . \tag{8}$$

C_{12} provides a scale for the intensity correlations. The lower bound $C_{12}=0$ means the two beams are uncorrelated. The upper bound $|C_{12}|=\sqrt{S_1S_2}$ means the fluctuations δp_1 and δp_2 are proportional, such as when the two beams are perfectly correlated ($\delta p_1=\delta p_2$, $C_{12}=S_1=S_2$) or when they are perfectly anticorrelated ($\delta p_1=-\delta p_2$, $C_{12}=-S_1=-S_2$).

From Eq. (4), the noise control of beam 1 can be written in terms of the spectra

$$\tilde{S}_1(\Omega)=S_1(\Omega)+|G(\Omega)|^2S_2(\Omega)-2\,\mathrm{Re}[G(\Omega)C_{12}(\Omega)]\ . \tag{9}$$

It is apparent here that S_i and C_{12} provide sufficient information on the two beams to determine the possible effectiveness of noise control. The maximum obtainable noise reduction in beam 1 at a frequency Ω is derived by minimizing $\tilde{S}_1(\Omega)$ as a function of the complex gain $G(\Omega)$. One finds

$$\tilde{S}_1^{\,\mathrm{opt}}(\Omega)=\frac{S_1(\Omega)S_2(\Omega)-|C_{12}(\Omega)|^2}{S_2(\Omega)} \tag{10a}$$

for an optimum transfer gain

$$G^{\mathrm{opt}}(\Omega)=\frac{C_{12}^*(\Omega)}{S_2(\Omega)}\ . \tag{10b}$$

We note here that the noise reduction can be perfect when $|C_{12}|$ is at its upper bound $\sqrt{S_1S_2}$, for example, when the two beams are initially perfectly correlated. On the other hand, if the two beams are initially uncorrelated ($C_{12}=0$), then the optimum gain is equal to zero, leaving the noise spectrum unchanged. It is best not to bother with control in this case since it is impossible to effect any noise reduction.

B. Balanced beams

In this section, we restrict ourselves to the simplifying assumption that beams 1 and 2 have symmetrical properties; that is, they are of equal intensities ($I_1=I_2=I$), equal intensity noise spectra ($S_1=S_2\equiv S$), and their correlations are symmetrical ($C_{12}=C_{21}$). We will denote these "balanced" beams. From Eqs. (7) and (10b), one observes that $C_{12}(\Omega)$ and $G^{\mathrm{opt}}(\Omega)$ become real functions.

A convenient correlation parameter is the noise spectrum $S_{1-2}(\Omega)$ of the intensity difference between the two beams, normalized to its associated shot-noise level

$$S_{1-2}(\Omega)=\langle\delta p_-(-\Omega)\delta p_-(\Omega)\rangle\ , \tag{11a}$$

where

$$\delta p_-(\Omega)=[\delta p_1(\Omega)-\delta p_2(\Omega)]/\sqrt{2}\ . \tag{11b}$$

This is easily measurable and, for the case of balanced beams, is simply related to $C_{12}(\Omega)$ by

$$S_{1-2}(\Omega)=S(\Omega)-C_{12}(\Omega)\ . \tag{12}$$

Quantum correlations between the two beam intensities correspond to $S_{1-2}(\Omega)<1$. Equation (9) for the noise spectrum after correction can now be written

$$\tilde{S}_1(\Omega)=[1-\mathrm{Re}(G)]^2 S(\Omega)+2\,\mathrm{Re}(G)S_{1-2}(\Omega)+\mathrm{Im}(G)^2 S(\Omega)\ . \tag{13}$$

One observes that, for a positive $\mathrm{Re}(G)$, the noise $\tilde{S}_1$ after correction is the sum of three positive terms. The first term represents the incident intensity noise S, attenuated by the control mechanism. This vanishes when $\mathrm{Re}(G)$ is set to 1. The second term represents a contamination noise introduced by the correction mechanism. This noise is proportional to $\mathrm{Re}(G)$ and stems from the decorrelation between the incident beams. The last term represents an additional contamination noise due to the dephasing of G with respect to G^{opt}.

The optimum gain and optimum noise reduction are then derived:

$$G^{\mathrm{opt}}(\Omega)=1-\frac{S_{1-2}(\Omega)}{S(\Omega)}\ , \tag{14a}$$

$$\tilde{S}_1^{\mathrm{opt}}(\Omega)=2S_{1-2}(\Omega)\left[1-\frac{S_{1-2}(\Omega)}{2S(\Omega)}\right]\ . \tag{14b}$$

When the excess noise in each beam is large $[S(\Omega)\gg 1]$, the optimum gain is equal to one and the optimally corrected intensity noise simply becomes $\tilde{S}_1^{\mathrm{opt}}(\Omega)=2S_{1-2}(\Omega)$. An initial quantum correlation of at least 50% $[S_{1-2}(\Omega)<0.5]$ is then necessary to obtain noise in the corrected beam below the shot-noise level. If the beams are not initially correlated at the quantum level $[S_{1-2}(\Omega)\geq 1]$, then the control mechanism cannot correct below the shot noise and reacts only on the classical excess noise in beam 1.

When the excess noise in each beam is small $[S(\Omega)\approx 1]$, noise levels less than $2S_{1-2}(\Omega)$ can be reached for optimum gains smaller than 1. An initial quantum correlation of at least 50% is no longer necessary for the sub-shot-noise correction.

These results can be understood alternatively by separating the beam fluctuations into their symmetric $[\delta p_+=(\delta p_1+\delta p_2)/\sqrt{2}]$ and antisymmetric (δp_-) components. One then finds

$$\tilde{S}_1(\Omega)=[|1-G|^2 S_{1+2}(\Omega)+|1+G|^2 S_{1-2}(\Omega)]/2\ , \tag{15}$$

where $S_{1+2}(\Omega)$ is the noise spectrum of the symmetric fluctuations δp_+, defined in the same way as in Eq. (11a). The fluctuations in beam 1 can be reduced to zero by subtracting the incident fields from one another $(G=1)$ when they are perfectly correlated $(\delta p_-=0)$, or by adding them $(G=-1)$ when they are anticorrelated $(\delta p_+=0)$. For intermediate cases when the beams are neither perfectly correlated nor perfectly anticorrelated, such a subtraction or addition of the two fields leaves a residual noise in beam 1 equal, respectively, to twice the symmetric or antisymmetric noises. In general, this is not the optimal noise reduction. The noise can optimally be reduced further by making a compromise $(|G|<1)$, leaving a residual noise in beam 1 containing both symmetric and antisymmetric noise components.

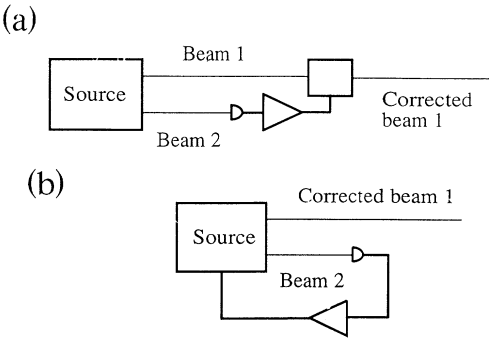

FIG. 1. Examples of control configurations using two light beams: the intensity of beam 2 is monitored and regulates the intensity fluctuations of beam 1 either (a) by direct feedforward control or (b) by indirect feedback control to the source.

C. Examples of control mechanisms

Two general classes of control configurations will be examined: those where the control is effected after the two fields have been generated (feedforward correction) and those where the control is effected retroactively at their source (feedback correction). Particular examples where the transfer channels are optoelectronic are shown in Fig. 1. The transfer function $G(\Omega)$ comprises a transfer of intensity fluctuations to voltage fluctuations by detection of beam 2, a voltage gain, and a transfer of voltage fluctuations back to intensity fluctuations by analog modulation of beam 1 either downstream or at its source. Such channels are easily realizable in practice and will be elaborated on at length in Sec. IV. In the present section, we examine the validity of the idealized model presented above [Eq. (4)] by outlining some examples of its implementation.

We turn first to a feedforward configuration, and adopt a simple transfer mechanism where beam 1 is subject to a transmission proportional to the measured intensity of beam 2. Such a loss can be modeled as a simple beam splitter with a variable transmission t:

$$t=\bar{t}-g\delta p_2\ , \tag{16}$$

where $\bar{t}$ is the bias of the beam splitter $(\bar{t}<1)$ and g the gain of the control mechanism. In a semiclassical analysis, the incoming fluctuations δp_1 are coupled to the vacuum fluctuations δp_v entering through the unused input port of the beam splitter (see Fig. 2). The resultant

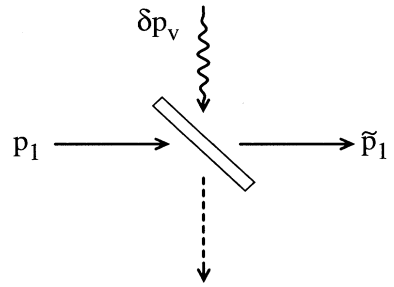

FIG. 2. Beam splitter model: outgoing field $\tilde{p}_1$ is the sum of incident field p_1 partly transmitted and vacuum fluctuations δp_v partly reflected.

outgoing fluctuations are

$$\delta\tilde{p}_1 = \bar{t}\delta p_1 - g|\alpha_1|\delta p_2 + r\delta p_v \ , \tag{17}$$

where $r=\sqrt{1-\bar{t}^2}$ is the reflection coefficient of the beam splitter.

This differs from the idealized model [Eq. (4)] in that beam 1 is attenuated by the bias $\bar{t}$ and there is an additional noise term [last term in Eq. (17)] associated with the losses in beam 1. Although the reflection coefficient r cannot be chosen arbitrarily small since the total transmission t [Eq. (16)] must be smaller than 1, it can be chosen of the order $g\Delta p_2 \approx \Delta p_1/|\alpha_1|$. The last term in Eq. (17) becomes negligible then and one recovers our idealized model.

The implementation of a feedback configuration is more complicated since it is necessary to consider the details of the beams' source. A general case is examined where we assume both beams are derived from a single driving field α_0. In a linear fluctuation analysis, the amplitude fluctuations of the beams are related then to those of the driving field δp_0 through linear transfer functions A_i:

$$\delta p_i = A_i\delta p_0 + \pi_i \quad (i=1,2) \ , \tag{18}$$

where π_i are other possible noise sources uncorrelated with δp_0. Such a transfer is found, for example, in the case of parametric downconversion (see Sec. III).

An identical mechanism to that described above is considered for the transfer of fluctuations from beam 2 to the driving beam. The amplitude fluctuations δp_0 in Eq. (18) then become

$$\delta p_0 \rightarrow \bar{t}\delta p_0 - g|\alpha_0|\delta p_2 + r\delta p_v \ . \tag{19}$$

One can relate the fluctuations $\delta\tilde{p}_1$, $\delta\tilde{p}_2$ with feedback ($g\neq 0$) to the fluctuations δp_1, δp_2 without feedback ($g=0$):

$$\delta\tilde{p}_1 = \delta p_1 - \frac{gA_1|\alpha_0|}{1+gA_2|\alpha_0|}\delta p_2 \ , \tag{20a}$$

$$\delta\tilde{p}_2 = \frac{1}{1+gA_2|\alpha_0|}\delta p_2 \ . \tag{20b}$$

One observes that, for large gains g, the amplitude fluctuations in beam 2 are completely attenuated by the feedback control. This is not necessarily the case for beam 1 where the amplitude fluctuations are attenuated only to the extent that the two beams are correlated. The effect of feedback on beam 1, however, is the same as that described by our idealized model [Eq. (4)], independent of the noise terms introduced by the source (π_i) or by the transfer mechanism (δp_v). The feedback configuration therefore presents a relative advantage over the feedforward configuration that the transmission $\bar{t}$ can be arbitrary.

D. Channel imperfections

Additional refinements can be made to our idealized model by including such imperfections as a nonideal quantum efficiency η in detector 2, and transfer channel noise. Loss in the detector is treated in the same manner as before, as a beam splitter of transmission $\sqrt{\eta}$, and channel noise is treated by including additional fluctuations δp_e at the input of the control mechanism, characterized by a power spectrum S_e. The measured fluctuations δp_2 are modified to

$$\delta p_2 \rightarrow \sqrt{\eta}\delta p_2 + \sqrt{1-\eta}\delta p_v + \delta p_e \ , \tag{21}$$

where δp_v represents the vacuum fluctuations coupled through the detector loss. From Eq. (4), the effect of control becomes

$$\delta\tilde{p}_1 = \delta p_1 - \sqrt{\eta}G\delta p_2 - \sqrt{1-\eta}G\delta p_v - G\delta p_e \ , \tag{22a}$$

$$\tilde{S}_1 = S_1 + \eta|G|^2S_2 - 2\,\mathrm{Re}(\sqrt{\eta}GC_{12}) + (1-\eta)|G|^2 + |G|^2S_e \ . \tag{22b}$$

Both refinements have the similar effect of introducing additional noise terms in beam 1. These are the last two terms in Eq. (22b), associated, respectively, with nonideal detector efficiency and channel noise. In addition, the gain G becomes effectively reduced by the factor $\sqrt{\eta}$, due to the loss incurred by beam 2.

The results derived from the previous sections still remain valid except that S_2 must be replaced by an effective spectrum:

$$S_2 \rightarrow S_2 + \frac{1-\eta}{\eta} + \frac{S_e}{\eta} \tag{23}$$

and G modified to $G/\sqrt{\eta}$. One finds the expected result that imperfections in the control channel tend to deteriorate the amount of attainable noise reduction.

III. APPLICATION TO TWIN BEAMS GENERATED BY OPO

We now consider an application of the above results, where beams 1 and 2 are generated by an optical parametric oscillator comprising a nonlinear medium inserted in an optical cavity (see Fig. 3). A theoretical model is presented in this section for the operation of the OPO. We use the semiclassical formulation which is well adapted for treating the OPO as a quantum network where incoming mode fluctuations are transferred to outgoing modes.

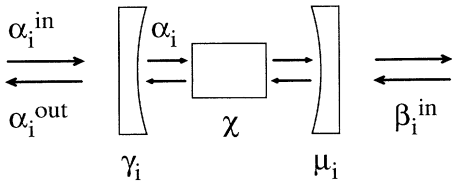

FIG. 3. Model of an optical parametric oscillator: a nonlinear medium (second-order susceptibility χ) is placed in an optical cavity with port mirror reflection coefficient $1-\gamma_i$ ($i=0$, 1, 2 for pump, signal, and idler modes). α_i^{in}, α_i, and α_i^{out} are, respectively, input, intracavity, and output fields. Losses are modeled by a back mirror reflection coefficient $1-\mu_i$ (input modes β_i^{in}).

We examine OPO operation in the nondegenerate regime where output modes 1 and 2 are separable either by frequency or polarization. The modes inside the cavity are coupled through a port mirror to the external output modes. Incoming mode 0 is the pump field channel and incoming modes 1 and 2 are assumed in the vacuum state, while outgoing modes 1 and 2 are the channels for beams 1 and 2 from Sec. II.

For small one-pass gain and losses, the semiclassical equations governing the field evolutions during a cavity round trip of time τ can be written as differential equations:

$$\tau\dot{\alpha}_0 = -2\chi\alpha_1\alpha_2 - \gamma_0'(1+i\varphi_0)\alpha_0 + \sqrt{2\gamma_0}\alpha_0^{\text{in}} + \sqrt{2\mu_0}\beta_0^{\text{in}} , \tag{24a}$$

$$\tau\dot{\alpha}_1 = 2\chi\alpha_0\alpha_2^* - \gamma_1'(1+i\varphi_1)\alpha_1 + \sqrt{2\gamma_1}\alpha_1^{\text{in}} + \sqrt{2\mu_1}\beta_1^{\text{in}} , \tag{24b}$$

$$\tau\dot{\alpha}_2 = 2\chi\alpha_0\alpha_1^* - \gamma_2'(1+i\varphi_2)\alpha_2 + \sqrt{2\gamma_2}\alpha_2^{\text{in}} + \sqrt{2\mu_2}\beta_2^{\text{in}} . \tag{24c}$$

The first terms on the right represent the parametric coupling due to the second-order susceptibility χ of the nonlinear medium. The second terms represent the field damping due, in part, to the port mirror (γ_i) and, in part, to extraneous intracavity losses (μ_i), where $\gamma_i' = \gamma_i + \mu_i$. The damping parameters γ_i are related to the transmission coefficients t_i of the port mirror through

$$t_i = \sqrt{2\gamma_i} \tag{25}$$

and μ_i are related similarly to a "transmission" of the second mirror which models all other loss mechanisms (see Fig. 3). Detuning is also included in Eqs. (24) where the phase shift from resonance of each field after a round trip is $\gamma_i'\varphi_i$. The last terms in Eqs. (24) represent the coupling to the external modes, respectively, through the port mirror (external modes α_i^{in}) and through the losses (external modes β_i^{in}).

The outgoing fields α_i^{out} are obtained simply from the superposition of the intracavity fields leaking out the port mirror and the incident fields reflected directly off the port mirror:

$$\alpha_i^{\text{out}} = \sqrt{2\gamma_i}\alpha_i - \alpha_i^{\text{in}} . \tag{26}$$

A. Stationary solutions for OPO

The stationary mean field solutions $\bar{\alpha}_i$ are obtained from Eqs. (24), noting that all the external mean fields are equal to zero except the pump $\bar{\alpha}_0^{\text{in}}$. When this pump is large enough, the solutions for $\bar{\alpha}_1$ and $\bar{\alpha}_2$ become nonzero and the OPO is set in oscillation. This oscillation imposes the restrictions that $\varphi_1 = \varphi_2 = \varphi$ and that the sum of the signal and idler phase is fixed. We neglect in this treatment the phase diffusion of each field taken individually since this occurs on time scales much longer than the fluctuation dynamics of interest [28]. A phase reference is chosen so that the stationary solutions for the intracavity signal and idler fields are real:

$$\bar{\alpha}_0 = \frac{\sqrt{\gamma_1'\gamma_2'}}{2\chi}(1+i\varphi) , \tag{27a}$$

$$\bar{\alpha}_1 = \frac{1}{2\chi}\sqrt{\gamma_0'\gamma_2'(\sigma-1)} , \tag{27b}$$

$$\bar{\alpha}_2 = \frac{1}{2\chi}\sqrt{\gamma_0'\gamma_1'(\sigma-1)} , \tag{27c}$$

where σ is a pump parameter related to the incident pump intensity $|\bar{\alpha}_0^{\text{in}}|^2$:

$$\sigma = \left[\frac{8\chi^2\gamma_0|\bar{\alpha}_0^{\text{in}}|^2}{\gamma_0'\gamma_1'\gamma_2'} - (\varphi_0+\varphi)^2\right]^{1/2} + \varphi_0\varphi . \tag{28}$$

These stationary solutions provide the working point about which the field fluctuations will be studied.

B. Field Fluctuations in OPO

The dynamics of the field fluctuations derive essentially from the linear expansion of Eqs. (24). Since the concern of this paper is the application of the OPO to single beam noise control, we skirt a general treatment of the OPO and adopt several simplifications. In particular, we assume the OPO is balanced ($\gamma_1 = \gamma_2 = \gamma$ and $\mu_1 = \mu_2 = \mu$). In this way, the output beams are also "balanced," as defined in Sec. II. In addition, we assume the pump is resonant with the cavity ($\varphi_0 = 0$), considered here in a bad cavity limit ($\gamma' \ll \gamma_0'$). These assumptions do not greatly affect the underlying physics but considerably simplify our analysis.

The intracavity fields are written in a symmetric and antisymmetric form

$$\alpha_\pm = (\alpha_1 \pm \alpha_2)/\sqrt{2} \tag{29}$$

and the rate equations for the intracavity fields conveniently separate into

$$\tau\delta\dot{\alpha}_+ = -2\gamma'(i-\varphi)\text{Im}(\delta\alpha_+) - \lambda\delta\alpha_+ + \sqrt{2\gamma}\delta\alpha_+^{\text{in}} + \sqrt{2\mu}\delta\beta_+^{\text{in}} + \sqrt{2\lambda}\delta\alpha_p^{\text{in}} , \tag{30a}$$

$$\tau\delta\dot{\alpha}_- = -2\gamma'(1+i\varphi)\text{Re}(\delta\alpha_-) + \sqrt{2\gamma}\delta\alpha_-^{\text{in}} + \sqrt{2\mu}\delta\beta_-^{\text{in}} , \tag{30b}$$

where $\lambda = 2\gamma'(\sigma-1)$ characterizes the parametric coupling to the pump mode and

$$\delta\alpha_p^{\text{in}} = \sqrt{(\gamma_0/\gamma_0')}\delta\alpha_0^{\text{in}} + \sqrt{(\mu_0/\gamma_0')}\delta\beta_0^{\text{in}} . \tag{31}$$

An advantage of these equations is that the incident fluctuations are all uncorrelated with one another. The symmetric and antisymmetric components of the fields can therefore be treated independently (see Fig. 4).

The intracavity fields are coupled to external modes via three channels, admitting the vacuum fluctuations $\delta\alpha_\pm^{\text{in}}$ through the port mirror, the vacuum fluctuations $\delta\beta_\pm^{\text{in}}$ through the other intracavity losses, and the fluctuations in the pump modes $\delta\alpha_p^{\text{in}}$ through the parametric conversion process. The intracavity fluctuations are driven only by these incident fluctuations. This differs from the standard quantum treatment of the OPO where the intracavi-

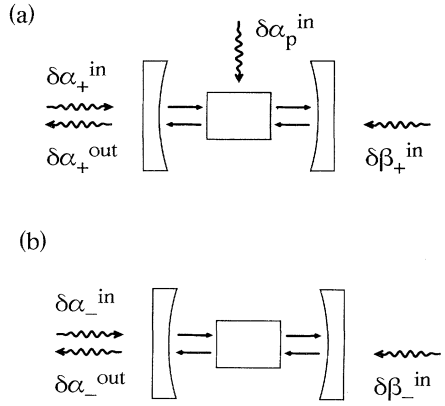

FIG. 4. Input-output model for the (a) symmetric and (b) antisymmetric field fluctuations. Output fluctuations $\delta\alpha_{\pm}^{out}$ are driven by input vacuum fluctuations $\delta\alpha_{\pm}^{in}$ (port mirror) and $\delta\beta_{\pm}^{in}$ (extra cavity losses), and by pump fluctuations $\delta\alpha_p^{in}$ through the parametric conversion process (symmetric case only).

ty fluctuations are said to originate entirely from the nonlinear medium [27,29]. With Eq. (26) relating the output field to the input and intracavity fields, the OPO can be viewed as a quantum network where input fluctuations are transferred to output fluctuations.

By separating the complex fields into column matrices $[\delta\alpha_r, \delta\alpha_i]$ with real and imaginary components, and taking the Fourier transform, Eqs. (30) become

$$[\delta\alpha_+^{out}]=(\sqrt{2\gamma}C_+-1)[\delta\alpha_+^{in}] +\sqrt{2\mu}C_+[\delta\beta_+^{in}]+\sqrt{2\lambda}C_+[\delta\alpha_p^{in}]\ , \tag{32a}$$

$$[\delta\alpha_-^{out}]=(\sqrt{2\gamma}C_--1)[\delta\alpha_-^{in}]+\sqrt{2\mu}C_-[\delta\beta_-^{in}]\ , \tag{32b}$$

where the coefficients multiplying each column matrix are the transfer functions for the separate input fluctuations. The matrices $C_{\pm}$ are defined here as

$$C_+=\frac{\sqrt{2\gamma}}{(2\gamma'\sigma+i\Omega\tau)(\lambda+i\Omega\tau)}\begin{bmatrix}2\gamma'\sigma+i\Omega\tau & 2\gamma'\varphi\\ 0 & \lambda+i\Omega\tau\end{bmatrix}, \tag{33a}$$

$$C_-=\frac{\sqrt{2\gamma}}{i\Omega\tau(2\gamma'+i\Omega\tau)}\begin{bmatrix}i\Omega\tau & 0\\ -2\gamma'\varphi & 2\gamma'+i\Omega\tau\end{bmatrix}. \tag{33b}$$

We note here that the intracavity and output mean fields are of the same phase. The real and imaginary components of their fluctuations therefore correspond to the quadrature components in phase (amplitude component δp) and out of phase (phase component δq) with the mean fields.

It is apparent from the above equations that both quadratures of the fluctuations remain uncoupled on resonance ($\varphi=0$) during the transfer process and are subject to simple low pass filtering in the cavity with differing time constants. At frequencies above the cavity bandwidth, $C_{\pm}$ tends towards zero and the output fluctuations tend towards the vacuum level. The output fluctuations are attributable then only to those input contributions not subject to cavity filtering; that is, the vacuum fluctuations reflected directly off the port mirror.

The effects of being off resonance ($\varphi\neq 0$) are a reduction in the pump parameter σ [Eq. (28)], and a mixing of the filed quadratures. It can be shown that these increase the symmetric intensity noise in general but leave the antisymmetric intensity noise unchanged.

The relevant spectra from Sec. II are determined from Eqs. (32). When all input fluctuations correspond to vacuum fluctuations, one finds

$$S=(\overline{|\delta p_+|^2}+\overline{|\delta p_-|^2})/2 =1+\frac{8\gamma\gamma'^3}{4\gamma'^2(\sigma-1)^2+\Omega^2\tau^2} \times\left[\frac{\sigma(2-\sigma)}{4\gamma'^2+\Omega^2\tau^2}+\frac{\varphi^2(2\sigma-1)}{4\gamma'^2\sigma^2+\Omega^2\tau^2}\right], \tag{34a}$$

$$S_{1-2}=\overline{|\delta p_-|^2}=1-\frac{4\gamma\gamma'}{4\gamma'^2+\Omega^2\tau^2}\ . \tag{34b}$$

The intensity difference spectrum S_{1-2} is independent of the pump and of detuning. At zero frequency, it is simply equal to the proportion μ/γ' of the cavity damping due to extraneous losses.

These results can be extended to include pump detuning ($\varphi_0\neq 0$) and cavity imbalance ($\gamma_1'\neq\gamma_2'$). The beams generated by the OPO are then no longer "balanced" and it is necessary to evaluate C_{12}. A general solution for the OPO operation may be derived in analytical form from Eqs. (24), using a method similar to the one presented above. It can be shown that C_{12} remains real at zero frequency. Furthermore, if the proportion of cavity damping due to extraneous losses is assumed constant ($\mu_1/\gamma_1'=\mu_2/\gamma_2'$), then $S_{1-2}(\Omega=0)$ remains independent of pump detuning and cavity imbalance, and equal to μ_1/γ_1'. One notes from Eqs. (2) and (11) that S_{1-2} is a measure of amplitude correlations and no longer of intensity correlations when the OPO is not balanced since the output beam intensities are no longer the same [19].

C. Single-beam control

It is straightforward to apply the expressions obtained above [Eq. (34)] to the results from Sec. II. One then finds the maximum noise reduction attainable for a single beam as a function of the OPO parameters (see Fig. 5). This maximum is valid regardless of whether the control is feedforward or feedback. In a feedforward configuration, the intensity of beam 2 is monitored and used directly to control the intensity noise of beam 1. In a feedback configuration, the control is more complicated. Since the output fluctuations of the OPO are functions of the well-identified input fluctuations, and since the input fluctuations from the pump beam in particular are readily accessible, a feedback loop can be realized where the output intensity fluctuations monitored at the output beam 2 are regulated by adjusting the intensity fluctuations of the pump. This has the effect of compensating not only the pump input fluctuations but all the other input fluctuations as well (to within the feedback

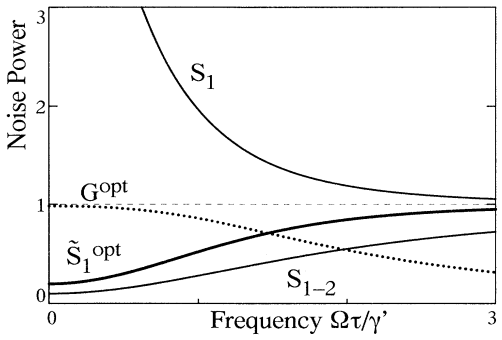

FIG. 5. Optimal noise control for twin beams generated by a balanced, tuned OPO ($\sigma=1.3$, $\gamma/\gamma'=0.9$). $S_1(\Omega)$ and $S_{1-2}(\Omega)$ are single-beam noise and intensity difference spectra. $\tilde{S}_1^{opt}(\Omega)$ is the noise spectrum after control using optimal transfer gain $G^{opt}(\Omega)$. Ω is normalized to the cavity half-bandwidth γ'/τ.

bandwidth), producing the same results as a direct feedforward control.

From Eqs. (32), one notes that feedback to the pump acts only on the symmetric noise and not the antisymmetric noise of each beam. It is interesting to consider then why such a feedback cannot, in general, completely eliminate this symmetric noise, thereby reducing the noise in beam 1 to S_{1-2}. The difficulty is that both the symmetric and antisymmetric output noise components are registered from beam 2. These are transferred to the pump beam by the feedback mechanism and even though the pump beam acts only on the symmetric noise, it contains deleterious information on the antisymmetric noise. In effect, the more one tries to correct the output symmetric noise, the more one contaminates it with antisymmetric noise. A compromise must be made, in general, for an optimum. In the limit where one tries to completely correct the symmetric noise, as in Fig. 5 where it is dominant at low frequencies, one ends with twice the antisymmetric noise in the controlled output beam, whereby $\tilde{S}_1^{opt}$ tends towards $2S_{1-2}$.

In general, signal or pump detunings (φ, $\varphi_0\neq 0$) and cavity imbalance ($\gamma_1'\neq\gamma_2'$) produce only little effect on single-beam control. This may be seen, for example, in Fig. 6 where $\tilde{S}_1^{opt}$ is displayed as a function of cavity imbalance. One observes that, at zero frequency, the optimum noise is left unchanged. Since single-beam excess noise is large, $\tilde{S}_1^{opt}$ is related only to S_{1-2}, and independent of cavity imbalance at zero frequency (see discussion above). At higher frequencies, $\tilde{S}_1^{opt}$ tends to degrade as a result of a reduction in the bandwidth of the intensity correlations.

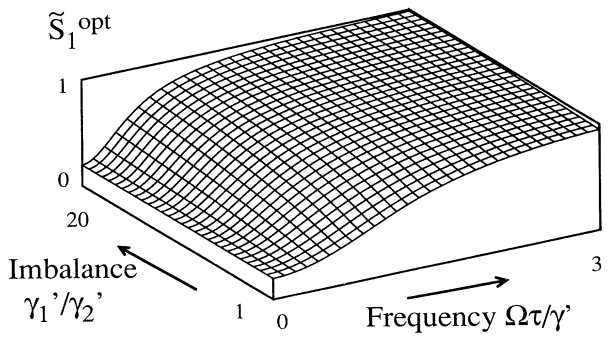

FIG. 6. Effect of cavity imbalance on optimally corrected noise spectrum $\tilde{S}_1^{opt}(\Omega)$. Imbalance of a tuned OPO ($\sigma=1.3$, $\gamma/\gamma'=0.9$) is varied for $\gamma'=\sqrt{\gamma_1'\gamma_2'}$ held constant.

An additional effect of cavity imbalance is that C_{12} becomes complex at nonzero frequencies. This may be interpreted as a frequency-dependent time delay between the two output beams, linked to their different cavity storage times. From Eq. (10b), one finds that the optimal control gain must be complex as well and of phase opposite to C_{12}. This reflects the intuitive result that for the reduction in noise to be optimal, the control mechanism must compensate for the time delay between the output beams by introducing its own supplementary time delay on the monitor beam. Of course, for this mechanism to be causal, the monitor beam must be chosen as the output beam with the shortest intracavity storage time.

IV. PRACTICAL REALIZATION OF BEAM CONTROL USING OPO

We examine here the implications of a realistic control channel on noise reduction. For noise reduction to be optimal, such a channel must be tailored to produce a global control gain $G^{opt}(\Omega)$. Unfortunately, it is often impractical or even impossible to realize such a fit over all frequencies, and, in general, one must settle for optimal noise control only over a limited bandwidth. We first study the limitations imposed by a stability analysis. We outline a specific realization of a control channel, delineating, in turn, the relative advantages and disadvantages of both configurations feedback and feedforward. Finally, we will discuss the results of our recent experimental study where we used a feedforward configuration.

A. Stability analysis

To illustrate the essential features of a control channel, we consider the simplified model where it comprises only a gain g, a simple filter of roll-off frequency Ω_0, and a time delay τ_d. The transfer function $H(\Omega)$ for this channel is

$$H(\Omega)=\frac{g\Omega_0 e^{-i\Omega\tau_d}}{\Omega_0+i\Omega} . \tag{35}$$

A standard method for analyzing the stability of the resultant control is to analytically continue $G(\Omega)$ into the complex Ω plane and follow the location of its poles. If all the poles are in the upper half-plane (uhp), the control is stable. If a single pole falls on the real frequency axis, the system is set into oscillation. Poles in the lower half-plane are forbidden by causality.

When our simple model is applied in a feedforward configuration, that is, when $G(\Omega)=H(\Omega)$, the control is always stable. The poles of $G(\Omega)$ lie in the uhp and remain fixed there independent of g. We illustrate this in Fig. 7(a) for the case of a balanced, tuned OPO, where $G^{opt}(\Omega)$ is real. It is clear that the bandwidth over which

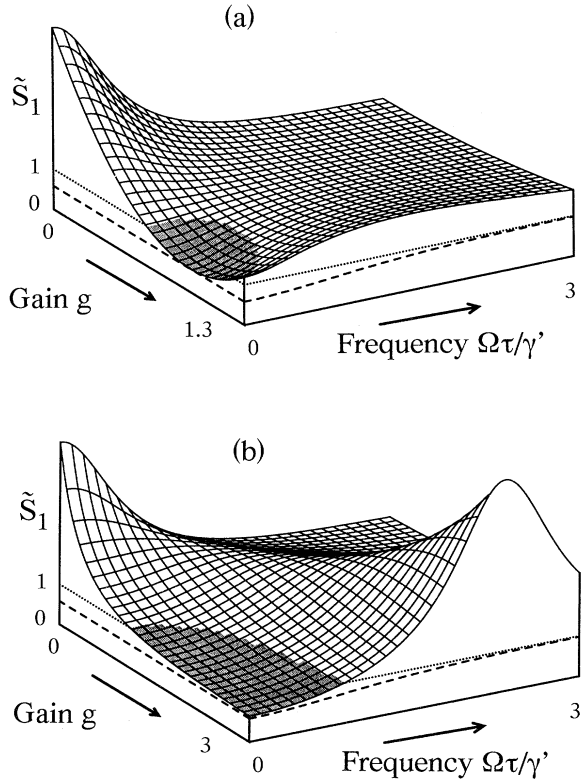

FIG. 7. Corrected noise spectra $\tilde{S}_1(\Omega)$ for (a) feedforward and (b) feedback configurations using a control channel comprising a gain g, a low-pass filter (roll-off frequency $\Omega_0=2\gamma'/\tau$), and a time delay ($\tau_d=0.25\tau/\gamma'$). OPO is tuned and balanced ($\sigma=1.3$, $\gamma/\gamma'=0.7$) Dashed curves represent the optimum noise reduction $\tilde{S}_1^{\text{opt}}$ for comparison. Shaded regions correspond to noise reduction below the shot-noise level. Ω is normalized to the cavity half-bandwidth γ'/τ.

the noise control is near optimal is smaller than the bandwidth possible in theory. The noise control becomes optimal only at low frequencies where $G(\Omega)$ is also real, and only for a specific value of g. We note that this optimum may be shifted to nonzero frequencies with more complicated control channels.

In a feedback configuration, on the other hand, $G(\Omega)$ comprises both the transfer from beam 2 to the pump through the control channel and the transfer from the pump to beam 1 through the OPO cavity. As in Sec. II, we ascribe to the latter the transfer function $A(\Omega)$ [see Eq. (18)]. From Eq. (32a), one finds, for the example of a balanced, tuned OPO,

$$A(\Omega)=\frac{\sqrt{2\gamma\gamma_0\lambda/\gamma_0'}}{\lambda+i\Omega\tau}\ , \tag{36}$$

where $A(\Omega)$ takes the form of a simple filter with roll-off frequency λ/τ. For pumping close to threshold where λ tends towards zero, this filter is dominant over the control channel filter.

Referring then to Eq. (20a), the global transfer function for feedback control becomes

$$G(\Omega)=\frac{A(\Omega)H(\Omega)}{1+A(\Omega)H(\Omega)}\ . \tag{37}$$

The pole locations of $G(\Omega)$ are this time manifestly dependent on g. For small gains, they are in the uhp and the feedback loop is stable. For larger gains, the poles are displaced and become "nudged" by even the slightest time delay τ_d towards the real axis. At a critical gain, the loop is set into oscillation. This sets an upper limit on the gain allowed in a feedback configuration. Illustrations of noise reduction using feedback with our simple channel model are shown in Fig. 7(b). The onset of oscillation is apparent. In many cases the maximum gain that is allowed before oscillation is not sufficient for the noise reduction in beam 1 to approach optimal. This maximum gain is largely governed by the location of the poles of filters $A(\Omega)$ and $H(\Omega)$. The lower these poles are in frequency, the lower the frequency of oscillation and, in general, the lower this maximum gain. For effective noise reduction, therefore, it is important to keep these pole locations at high frequencies. This usually entails maximizing the OPO parameter λ/τ or working with fast electronics.

B. Feedforward versus feedback

It was shown in Sec. II that the transfer of fluctuations from one beam to another is possible using a variable attenuator. In practice, such an attenuator might consist of an electro-optic modulator followed by a polarizer. The intensity fluctuations in beam 2 are registered as voltage fluctuations which then pilot the attenuator transmission and modify the intensity fluctuations in either the pump beam or beam 1. A side effect of this type of channel is that it also modifies the phase fluctuations of the controlled beam. This may pose a problem in a feedback configuration since the phase fluctuations of the pump beam are mixed into the intensity fluctuations of the signal and idler beams when the OPO is detuned. One can circumvent this problem by inserting into beam 1 a second modulator+polarizer run in parallel with the first modulator+polarizer but with opposite polarity. The transfer to intensity fluctuations is doubled then, whereas the transfer to phase fluctuations is canceled.

An advantage of feedback control over feedforward control is that the transfer function $G(\Omega)$ is relatively insensitive to variations in g. As observed in Fig. 7(b), for example, it suffices for optimal control that g be large (albeit not so large that the system oscillates). This allows the noise control to be effective over a larger bandwidth than in a feedforward configuration, where g must take on a specific value.

A second advantage of feedback over feedforward is that beam 1 is left uncluttered of extraneous losses. It was shown in Sec. II that these losses could be reduced in theory to the point where the noise they introduced was negligible. This is often not the case, in practice, and, for a mean amplitude transmission $\bar{t}$ through the feedforward intensity modulator, the optimally reduced noise spectrum of beam 1 becomes degraded to $\bar{t}^2\tilde{S}_1+1-\bar{t}^2$.

A notable disadvantage of feedback, however, is its propensity towards oscillation. As illustrated in the

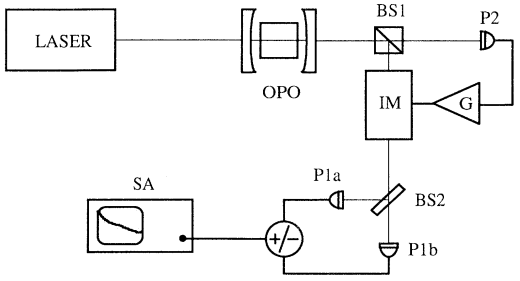

FIG. 8. Experimental layout: twin beams generated by an OPO are separated by beam splitter BS1. One beam is used to correct the intensity fluctuations of the other by active control (photodetector P2, amplifier G, and intensity modulator IM). BS2 is a 50% beam splitter and signals from photodiodes PA1 and PA2 are added or subtracted to measure respectively the intensity noise spectrum or shot-noise level of the corrected beam with spectrum analyzer SA.

above stability analysis, this imposes restrictions on the loop gain which hinder the effectiveness of the noise reduction. A feedback loop that is conditionally stable may be used to bypass these restrictions, obtaining higher gains below the oscillation frequency.

C. Observation of sub-shot-noise light using feedforward control

We now consider an experiment we recently performed using a feedforward configuration. Although the results of our experiment are presented in Ref. [17], emphasis will be made here on the technical aspects of the control channel.

The layout of the experiment is shown in Fig. 8. The twin output beams were approximately balanced (their mean intensities differed by less than 3%). The single-beam noise spectrum S_1 and the difference spectrum S_{1-2} are shown in Fig. 9. The maximum attainable noise reduction for beam 1 deduced from these spectra [using Eq. (14b)] is also shown in Fig. 9.

The feedforward channel in this experiment consisted of a low noise amplifier followed by an electro-optic intensity modulator presenting a total transmission loss in beam 1 of 20% (due to transmission biasing and intrinsic EOM losses). It is observed that the noise in each output beam was substantially above the shot-noise level at low frequencies, due to the fact that the OPO was pumped close to the threshold. A consequence of this large excess noise was that high-pass filters (12-dB roll off below 1 MHz) were required in the feedforward electronics to prevent amplifier saturation. A low-pass filter was inserted at 6 MHz along with the intrinsic amplifier roll off around 12 MHz resulting in zero-phase lag in the feedforward channel near 5 MHz. The overall gain was adjusted for optimal noise reduction at this frequency. For an initial beam correlation S_{1-2} at 5 MHz of 0.44, this noise reduction went as much as 24% below the shot-noise level (see Fig. 10). Given the parameters of the experiment, this result is in complete accord with theory.

The principal limitations of the channel used in this experiment were twofold. It is clear from the results that the bandwidth over which the noise reduction in beam 1 was effective is small compared with the bandwidth theoretically available. The primary reason for this is that the actual transfer function presented by the channel only fit the optimal transfer function $G^{\mathrm{opt}}(\Omega)$ over a limited frequency range, centered around 5 MHz. Deviations from this optimal occurred both in the magnitude of the transfer, which only approximately followed G^{opt}, and in its phase, which unavoidably varied with channel response. A second limitation imposed by the channel stemmed from the losses presented by the intensity modulator due in part to transmission bias. A higher transmission bias would have necessitated a higher feedforward gain, running again into the problem of amplifier saturation. The modulator loss resulted here in a degradation from a possible noise reduction of 30% to an actual noise reduction of 24% below the shot-noise level.

Possible improvements for this experiment are, of course, minimizing the effects of the above limitations; that is, better tailoring the feedforward electronics and

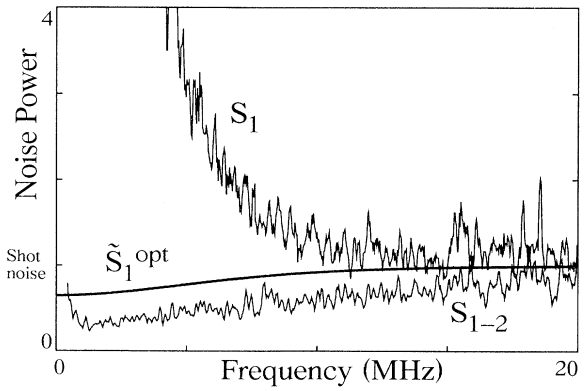

FIG. 9. Experimentally observed single-beam noise spectrum $S_1(\Omega)$ and intensity difference spectrum $S_{1-2}(\Omega)$ for twin beams out of OPO. $\tilde{S}_1^{\mathrm{opt}}(\Omega)$ represents the theoretically obtainable spectrum after optimal noise reduction deduced from these spectra. Scales are linear.

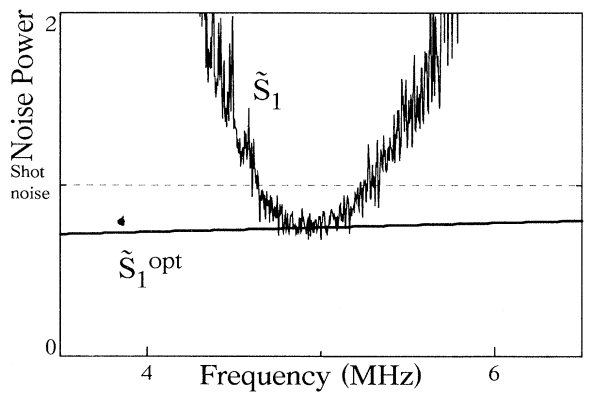

FIG. 10. Experimental noise spectrum $\tilde{S}_1(\Omega)$ using feedforward correction with OPO. $\tilde{S}_1^{\mathrm{opt}}(\Omega)$ represents the theoretically obtainable spectrum, taking into account optical losses. Scales are linear.

reducing the modulator loss. The feedback configuration also seems promising, and studies are underway to temper the effects of oscillation with improved OPO parameters and feedback electronics.

V. CONCLUSION

A theoretical optimum was determined for the amount of intensity noise reduction one can obtain when one beam of light is used to control another. It was found that the resultant noise spectrum of the controlled beam could be reduced to twice the intensity difference spectrum for beams with large excess noise, but that it could be reduced even further for beams with small excess noise. Conditions were determined for the generation of sub-shot-noise light using this control technique, both on the source of the two beams and on the control channel. Although we restricted our study to the case where the source was an OPO and the channel was electro-optic, the results we derived are general. They may be applied, for example, to all-optical channels or even to the case of a single beam where the control signal is provided by a QND measurement. OPO's present the experimental advantage, however, that they have already demonstrated their effectiveness in producing highly correlated light beams [30] which are easy to manipulate. This makes them particularly adapted for further studies of active noise control.

ACKNOWLEDGMENTS

We are grateful to S. Reynaud, E. Giacobino, L. Hilico, and T. Debuisschert for helpful discussions. This work was partially supported by EEC Contract No. ESPRIT BRA 3186, and one of us (J.M.) by DRET Contract JC No. 90/1333/A000. The Laboratoire de Spectroscopie Hertzienne is a "Laboratoire de l'Ecole Normale Supérieure et de l'Université Pierre et Marie Curie, associé au Central National de la Recherche Scientifique."

[1] S. Saito, O. Nilsson, and Y. Yamamoto, Appl. Phys. Lett. **46**, 3 (1985).
[2] S. Machida and Y. Yamamoto, Opt. Commun. **57**, 290 (1986).
[3] Y. Yamamoto, N. Imoto, and S. Machida, Phys. Rev. A **33**, 3243 (1986).
[4] H. Haus and Y. Yamamoto, Phys. Rev. A **34**, 270 (1986).
[5] H. Yuen, Phys. Rev. Lett. **56**, 2176 (1986).
[6] J. Shapiro, G. Saplakoglu, S. T. Ho, P. Kumar, B. Saleh, and M. Teich, J. Opt. Soc. Am. B **4**, 1604 (1987).
[7] E. Giacobino, C. Gabre, S. Reynaud, A. Heidmann, and R. Horowicz, in *Photons and Quantum Fluctuations,* edited by E. Pike and H. Walther (Hilger, Bristol, 1988), p. 81.
[8] G. Bjork and Y. Yamamoto, Phys. Rev. A **37**, 125 (1988).
[9] J. Walker and E. Jakeman, Opt. Acta **32**, 1303 (1985).
[10] B. Saleh and M. Teich, Opt. Commun. **52**, 429 (1985).
[11] E. Jakeman and J. Walker, Opt. Commun. **55**, 219 (1985).
[12] C. Hong and L. Mandel, Phys. Rev. Lett. **56**, 58 (1986).
[13] D. Stoler and B. Yurke, Phys. Rev. A **34**, 3143 (1986).
[14] J. Rarity, P. Tapster, and E. Jakeman, Opt. Commun. **62**, 201 (1987).
[15] P. Grangier, G. Roger, and A. Aspect, Europhys. Lett. **1**, 173 (1986).
[16] P. Tapster, J. Rarity, and J. Satchell, Phys. Rev. A **37**, 2963 (1988).
[17] J. Mertz, A. Heidmann, C. Fabre, E. Giacobino, and S. Reynaud, Phys. Rev. Lett. **64**, 2897 (1990).
[18] S. Reynaud and A. Heidmann, Opt. Commun. **71**, 209 (1989).
[19] C. Fabre, E. Giacobino, A. Heidmann, and S. Reynaud, J. Phys. (Paris) **50**, 1209 (1989).
[20] A. Heidmann, R. Horowicz, S. Reynaud, E. Giacobino, C. Fabre, and G. Camy, Phys. Rev. Lett. **59**, 2555 (1987).
[21] T. Debuisschert, S. Reynaud, A. Heidmann, E. Giacobino, and C. Fabre, Quantum Opt. **1**, 3 (1989).
[22] C. Nabors and R. Shelby, Phys. Rev. A **42**, 556 (1990).
[23] K. Leong, N. Wong, and J. Shapiro, Opt. Lett. **15**, 1058 (1990).
[24] S. Reynaud, Ann. Phys. (Paris) **15**, 63 (1990).
[25] C. Fabre and S. Reynaud, in *Fundamentals Systems in Quantum Optics,* Proceedings of the Les Houches Summer School of Theoretical Physics, 1990, edited by J. Dalibard, J. M. Raimond, and J. Zinn-Justin (Elsevier Science, British Vancouver, 1991).
[26] H. M. Gibbs, *Optical Bistability: Controlling Light with Light* (Academic, New York, 1985).
[27] C. Fabre, E. Giacobino, A. Heidmann, L. Lugiato, S. Reynaud, M. Vadacchino, and W. Kaige, Quantum Opt. **2**, 159 (1990).
[28] J. Y. Courtois, A. Smith, C. Fabre, and S. Reynaud, J. Mod. Opt. **38**, 177 (1991).
[29] P. D. Drummond, K. J. McNeil, and D. F. Walls, Opt. Acta **28**, 211 (1981).
[30] E. Giacobino, J. Mertz, T. Debuisschert, A. Heidmann, S. Reynaud, and C. Fabre, in *Proceedings of NATO ARW Quantum Measurements in Optics, Cortina, Italy, 1991* (Plenum, New York, in press).